Ellipsometry measurement of the complex refractive index and thickness of polysilicon thin films

Jau Hwang Ho, Chung Len Lee, Tan Fu Lei, and Tien Sheng Chao

Institute of Electronics, National Chiao Tung University, Hsinchu, Taiwan, China

Received May 1, 1989; accepted September 25, 1989

A scheme to measure precisely the complex refractive index, $N - iK$, and the thickness of polycrystalline silicon (poly-Si) film is proposed and demonstrated. The measurement is made by scanning the ellipsometer light beam along a beveled surface of the poly-Si film and by adopting a zero-layer model to derive the $N_{se} - T$ plot, where N_{se} is the equivalent real refractive index and T is the thickness of the measured poly-Si film. The complex refractive index, $N - iK$, is obtained from the $N_{se} - T$ plot, and the thickness is computed from the ellipsometry equation. Error analyses have been done on both the conventional ellipsometry method and the proposed method, and results show that the proposed method has more than an order-of-magnitude improvement in accuracy compared with the conventional method. Experimental results of applying this method to measure the complex refractive index of poly-Si films prepared at different processing conditions are also shown.

INTRODUCTION

Polycrystalline silicon (poly-Si) films have many important applications, such as gates, interconnects, and load resistors in integrated-circuit devices. Many characterization techniques, such as ellipsometry, scanning electron microscopy, transmission electron microscopy, and x ray, have been employed to analyze the fabricated poly-Si films.[1-4] Of these techniques, ellipsometry is one of the most effective because it is simple and nondestructive. When ellipsometry is applied to poly-Si films, however, there are several factors that make measurement difficult[2,5-9]: (1) The poly-Si film is absorptive of the incident light. More than two sets of measurement data on Δ and ψ are needed in order to deduce the values of the real part (N) and the imaginary part (K) of the refractive index. (2) The ellipsometric period for poly-Si is very small (approximately 850 Å for λ = 6328-Å light). Before measurement, the approximate film thickness must be known within 850 Å. (3) Poly-Si films usually have poor surface conditions. The roughness either on the surface native oxide or on the poly-Si films disturbs the characteristics of the reflected polarized light. (4) The errors in the ellipsometric parameters sometimes significantly affect the accuracy of the computed N and K.

Applications of ellipsometry to measure the refractive-index N and K were studied by Holmes and Feucht[10] and by Irene and Dong.[11] Holmes and Feucht proposed an approximate method, using a multiple-incident-angle ellipsometry, to measure the weakly absorbing poly-Si film in the 50-μm range, whose K value is less than 1% of the N value. Irene and Dong used the computed $\Delta - \psi$ chart to fit the measured Δ and ψ values to search for the N and K values for prepared poly-Si films. In these two studies, factors (3) and (4) above were not considered.

In this paper a scheme using ellipsometry to measure the values of N and K of poly-Si films more accurately is presented. This scheme greatly reduces the errors caused by factors (3) and (4) above. The N and K obtained are then used to compute the thickness T. To demonstrate the improvement in accuracy, the error sensitivities of N and K obtained by using the conventional method and the proposed method are computed and compared. The errors for the computed T are also analyzed. Some results of measurements of the N and K of poly-Si films that were prepared under different conditions are also presented to demonstrate this method.

ERROR SENSITIVITIES OF N AND K BY ELLIPSOMETRIC PARAMETERS

In order to demonstrate the improvement in accuracy for this proposed method, the error sensitivities of N and K obtained by using ellipsometric parameters are theoretically computed, based on a double-layer model. The double-layer model used in this study is shown in Fig. 1, where N_0, $N_1 - iK_1$, $N_2 - iK_2$, and $N_s - ik_s$ are the refractive indices of the ambient medium, the top surface layer, the bottom surface layer, and the substrate, respectively, and T_1 and T_2 are the thicknesses of the top surface layer and the bottom surface layer, respectively. For the model of Fig. 1, the conventional ellipsometric equations can be expressed as follows[12]:

$$f(\Delta, \psi, \phi_0, N_s, K_s, N_2, K_2, T_2, N_1, K_1, N_0, \lambda) = T_1, \quad (1)$$

$$g(\Delta, \psi, \phi_0, N_s, K_s, N_2, K_2, T_2, N_1, K_1, N_0, \lambda) = 0, \quad (2)$$

where Δ and ψ are the ellipsometric data and ϕ_0 and λ are the incident angle and the wavelength of the monochromatic light of the ellipsometer, respectively.

For this study the small deviations from the normal values of each ellipsometric parameter are listed in Table 1, along with the normal values. The refractive index of the top surface layer is assumed to be $3.80 - i0.05$, which is nearly equal to the refractive index of poly-Si films. The bottom surface layer is assumed to be a SiO_2 layer with $N_2 = 1.46 - i0.00$ and T_2 = 200 Å. The simulating layer, which is an equivalent layer with an equivalent refractive index N_e = 1.46 and an equivalent thickness T_e = 20 Å, simulates the

0740-3232/90/020196-10$02.00 © 1990 Optical Society of America

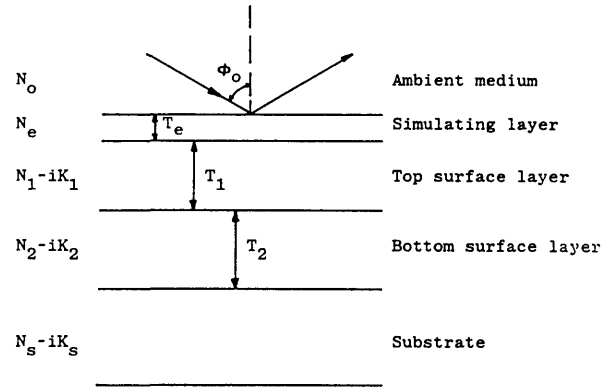

Fig. 1. Double-layer model for which the poly-Si surface layer and the sandwiched oxide layer are upon the substrate. A simulated layer, which simulates the native oxide layer or the rough surface of the poly-Si films, is on top of the poly-Si layer.

surface native oxide and the roughness of the poly-Si film mentioned above. It has been reported that this simulating layer is of the order of 15 to 70 Å (rms), depending on the processing conditions of the poly-Si film.[2]

From Eq. (2), the errors of N_1 are computed in terms of the film thickness, T_1, for various deviations in Δ, ψ, ϕ_0, N_s, K_s, N_0, T_2, K_1, and T_e. Since the errors caused by the deviations in Δ, ψ, ϕ_0, N_s, K_s, and N_0 are small, they are lumped into the rms error as $\delta\Sigma$. The error $\delta\Sigma$ and the errors caused by T_2, K_1, and T_e are plotted in Fig. 2 for $\hat{N}_1 = 3.80 - i0.05$. It is seen that the deviations in T_2, K_1, and T_e cause significant errors over the thickness range of 0–2000 Å. In particular, at thicknesses of 0, 400, and 800 Å, etc., which is the half of the ellipsometric period for the poly-Si for $\lambda = 6328$ Å, the errors are much greater.

The errors in K_1 caused by the deviations in those parameters are also computed as percentage errors (Fig. 3). The deviations in T_2, N_1, and T_e still cause large errors. The error $\delta\Sigma$ is negligible except in the thickness range <100 Å. In both Figs. 2 and 3, T_e, the stimulating layer, affects the accuracy significantly, as stated above. The accuracy of N_1 varies with the accuracy of K_1 and vice versa. Since both N_1 and K_1 are unknown and are to be computed, it can be expected that large errors could occur during computation of N_1 and K_1.

PROPOSED METHOD OF MEASURING *N* AND *K*

In this section a method for reducing errors in computing N and K is presented. First it is described qualitatively, and then a mathematical model to extract the N and K values is presented.

Description of the Method

In the proposed method an equivalent zero-layer model, which is derived from the single-layer model, is used. For the conventional single-layer model, there is a single surface layer upon the substrate. In the zero-layer model, the surface layer and the substrate are lumped into a simple equivalent substrate, which has an equivalent refractive index, $N_{se} - iK_{se}$, where N_{se} and K_{se} are the real part and the imaginary part, respectively, of the refractive index. $N_{se} - iK_{se}$ can be

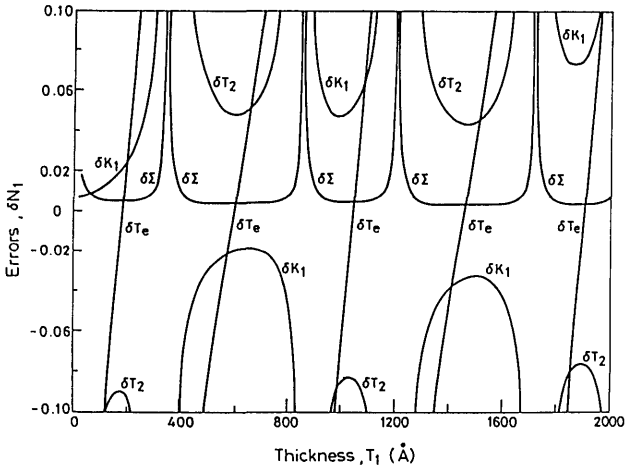

Fig. 2. Plots of the errors in N_1 due to various small deviations of $\delta\Sigma$, δK_1, δT_2, and δT_e for $\hat{N}_1 = 3.80 - i0.05$. $\delta\Sigma$ are the rms errors for $\delta\Delta$, $\delta\psi$, $\delta\phi_0$, δN_s, and δK_s.

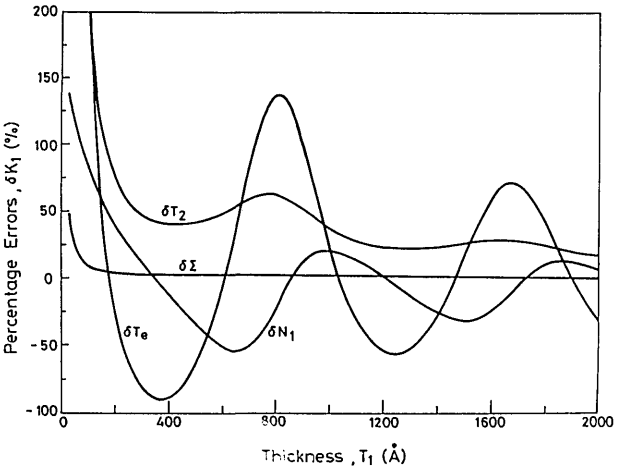

Fig. 3. Plots of the percentage errors in K_1 due to various small deviations of $\delta\Sigma$, δN_1, δT_2, and δT_e for $\hat{N}_1 = 3.80 - i0.05$. $\delta\Sigma$ are the rms errors for $\delta\Delta$, $\delta\psi$, $\delta\phi_0$, δN_s, and δK_s.

Table 1. Normal Values and Small Deviations in Each Parameter for the Double-Layer Model[a]

	Δ	ψ	ϕ_0	N_s	K_s	N_2	K_2	T_2	N_1	K_1	N_e	T_e	N_0
Normal values	—	–	70.00°	3.858	0.018	1.46	0.00	200 Å	3.80	0.05	1.46	0 Å	1.000
Deviations	1°/12	1°/24	0.02°	0.008	0.008	0	0	5%	0.05	0.01	0	20 Å	0.0003

[a] The values are taken for $\lambda = 6328$ Å.

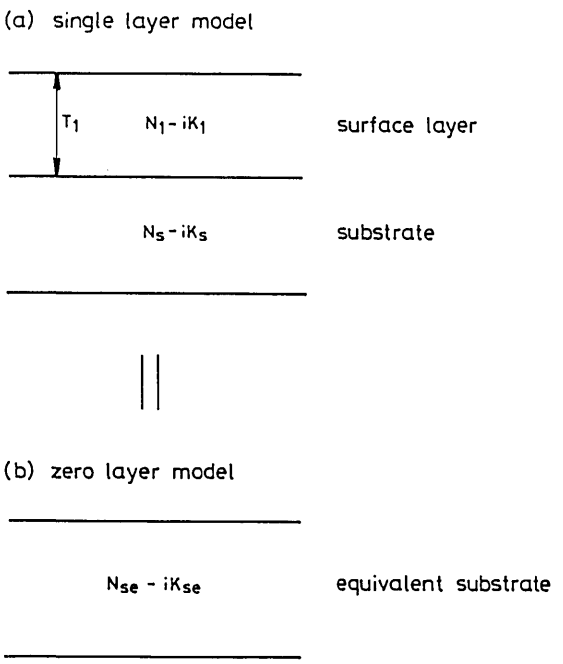

Fig. 4. (a) Conventional single-layer model. (b) A transformed equivalent zero-layer model, which is an equivalent substrate with an equivalent refractive index $N_{se} - iK_{se}$.

computed from the same (Δ, ψ) as those used for the single-layer model. Figures 4(a) and 4(b) show the single-layer model and the corresponding transformed equivalent zero-layer model, respectively.

The ellipsometric equations for the zero-layer model can be derived like those of the single-layer model:

$$f(\Delta, \psi, \phi_0, N_{se}, K_{se}, N_0, \lambda) = 0, \quad (3)$$

$$g(\Delta, \psi, \phi_0, N_{se}, K_{se}, N_0, \lambda) = 0. \quad (4)$$

Figure 5(a) is a computed plot of the equivalent N_{se} of the zero-layer model from a single-layer model in which the substrate has a refractive index $3.858 - i0.018$ and the surface layer has a thickness varying from 0 to 4000 Å but a refractive index of $N_1 = 3.50 - i0.00$. It is seen that the computed equivalent N_{se} varies periodically with the film thickness of the surface layer. From this curve it is seen that the average value of each adjacent minimum and maximum is close to the true refractive index N_1 of the single-layer model. A similar plot (the thin solid curve) of N_{se} derived from a single-layer model whose surface layer has a varying thickness but a refractive index of $\hat{N}_1 = 3.80 - i0.00$ has the same characteristics. The average of the adjacent minimum and maximum is 3.80, which is the true refractive index N_1 of the single-layer model.

In the above computation, if the refractive index has a nonzero imaginary part, i.e., the surface layer is an optical absorbing film, the computed equivalent N_{se} still exhibits a periodic characteristic, except that the amplitude of the curve gradually decays. A sample curve for the previous case when $N_1 = 3.50 - i0.10$ is also plotted [the dashed curve in Fig. 5(a)]. Compare this curve with the corresponding nonabsorbing curve; it can be seen that the maximum and the minimum of the curve shift toward the right slightly. An envelope that decreases in amplitude with the film thickness can be drawn for the absorbing curve. However, the average of the adjacent maximum and minimum is still close to 3.50, which is the real part of the true refractive index of the surface layer.

The above plots suggest a way to extract the refractive index, both the real part and the imaginary part, of a surface absorbing film; that is, the average of the plotted N_{se} of the equivalent zero-layer model gives the real part, N_1, and the decay of the curve gives the imaginary part, K_1, of the refractive index of the surface layer film.

Mathematic Model of the Extraction of N_1 and K_1

The extraction of N_1 and K_1 can be treated mathematically in a more rigorous way. From Fig. 5(a) it is seen that the N_{se}'s vary periodically with the film thickness. In Appendix A it is shown that, for poly-Si film upon a silicon substrate, the local maximum, $N_{se}(\max)$, and the local minimum, $N_{se}(\min)$, in this $N_{se} - T_1$ plot have the following approximate forms:

$$N_{se}(\max) = N_1 + (N_s - N_1)\exp[-2(m-1)\pi K_1/N_1], \quad (5)$$

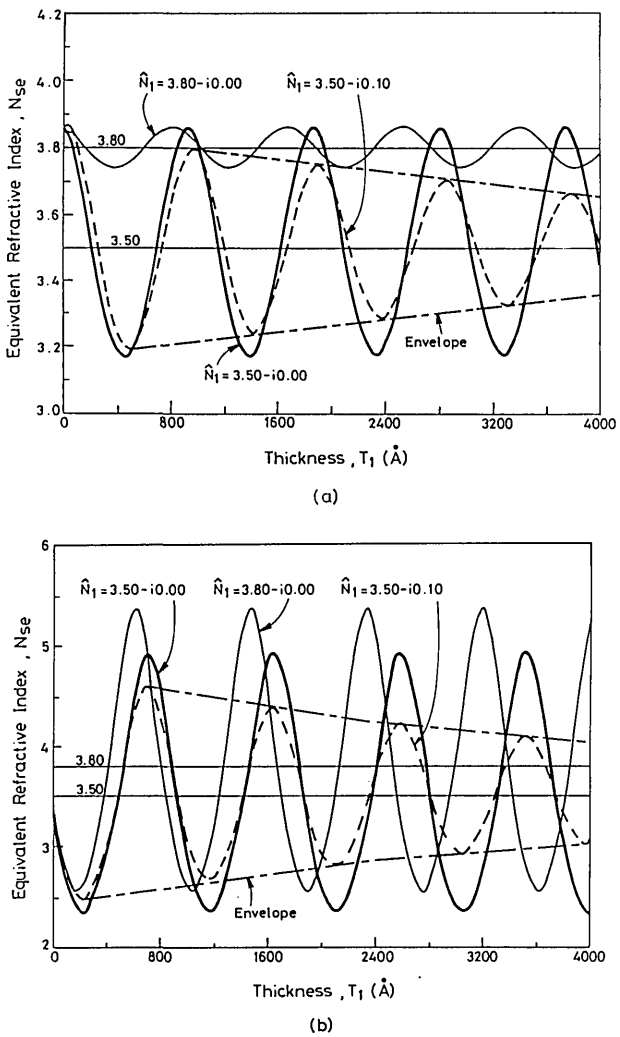

Fig. 5. Theoretical plots of N_{se} as functions of the thickness, T_1, for $\hat{N}_1 = 3.50 - i0.00$, $3.50 - i0.10$, and $3.80 - i0.00$, assuming that (a) $T_2 = 0$ Å and (b) $T_2 = 200$ Å.

$$N_{se}(\min) = N_1 - (N_s - N_1)\exp[-(2m-1)\pi K_1/N_1], \quad (5')$$

where $m = 1, 2, 3 \ldots$, which represents the mth local maximum or minimum. Equations (5) and (5′) can be expressed as

$$N_{se}(\max) = N_1 + \alpha \exp[-l\beta K_1/N_1], \qquad l = 0, 2, 4, \ldots, \quad (6)$$

$$N_{se}(\min) = N_1 - \alpha \exp(-l\beta K_1/N_1), \qquad l = 1, 3, 5, \ldots, \quad (6')$$

where α and β are constants. Equations (6) and (6′) indicate that K_1 can be extracted from the graph of the $\ln[N_{se}(\max) - N_1]$-versus-l plot or the $\ln[N_1 - N_{se}(\min)]$-versus-l plot. The slopes of these plots give the $-\beta K_1/N_1$ value, and then K_1 is obtained if N_1 is known.

Equations (5) and (5′) can be averaged to obtain

$$\frac{N_{se}(\max) + N_{se}(\min)}{2} = N_1 + \frac{(N_s - N_1)}{2}\exp(-m\pi K_1/N_1)[1 - \exp(-\pi K_1/N_1)], \quad (7)$$

which can be expressed as

$$\frac{N_{se}(\max) + N_{se}(\min)}{2} = N_1 + \Delta N, \quad (7')$$

where $\Delta N = [(N_s - N_1)/2]\exp(-m\pi K_1/N_1)[1 - \exp(-\pi K_1/N_1)]$. Equation (7′) indicates that N_1 can be determined from the neighboring maximum $N_{se}(\max)$ and minimum $N_{se}(\min)$ if K_1 is known. In Eq. (7′), ΔN is usually an order of magnitude smaller than N_1. Hence the error in N_1 obtained is influenced only little by the error in ΔN, i.e., the error in K_1. In practice, the error in N_1 can be reduced further by employing a numerical iteration procedure, which is described below, to extract N_1 and K_1.

The above analysis holds for a single-layer film. This method can be extended to a multiple-layer film since a multiple-layer film can be modified to be a single-layer film by lumping the surface layer with the substrate into an equivalent substrate with an effective refractive index. Figure 5(b) shows a $N_{se} - T_1$ plot computed for a three-layer structure, which is similar to the example in Fig. 5(a), where a thin SiO_2 layer with $\hat{N} = 1.46 - i0.00$ and $T = 200$ Å exists between the surface layer and the substrate. From Fig. 5(b) it can be seen that the average of the adjacent maximum and minimum is still close to the true refractive index of the surface layer, and for the $K \neq 0$ curve the envelopes also decrease in amplitude with the film thickness.

ANALYSIS OF ERRORS IN THE DETERMINATION OF N_1, K_1, AND T_1

One of advantages of the proposed method is that the errors in determining N_1, K_1, and T_1 are much reduced. In this section an error analysis of this scheme is studied.

Analysis of Errors in the Determination of K_1

As described above, in this method two or more $N_{se}(\max)$'s or $N_{se}(\min)$'s are used to determine the K_1 value by extracting the slope of the $\ln[N_{se}(\max) - N_1]$-versus-l plot or the $\ln[N_1 - N_{se}(\min)]$-versus-l plot. Assume that two $N_{se}(\max)$'s, i.e., N_{se1} and N_{se2}, are used to compute K_1. From Eq. (6) it is obtained that

$$N_{se1} = N_1 + \alpha \exp(-l_1\beta K_1/N_1), \quad (8)$$

$$N_{se2} = N_1 + \alpha \exp(-l_2\beta K_1/N_1). \quad (8')$$

From Eqs. (8) and (8′) the slope $-\beta K_1/N_1$ can be expressed as

$$-\beta\frac{K_1}{N_1} = \frac{\ln[(N_{se2} - N_1)/(N_{se1} - N_1)]}{(l_2 - l_1)}. \quad (9)$$

Taking the differentiation on Eq. (9), we obtain approximately

$$\delta K_1 = \gamma\left[\frac{\delta N_{se1}}{(N_{se1} - N_1)} - \frac{\delta N_{se2}}{(N_{se2} - N_1)}\right], \quad (10)$$

where $\gamma = N_1/[\beta(l_2 - l_1)]$. The terms δN_{se1} and δN_{se2} can also be expressed in terms of the deviations of parameters as

$$\delta N_{se1} = a_1{}^1\delta T_2 + a_2{}^1\delta N_1 + a_3{}^1\delta T_e + a_4{}^1\delta\Sigma, \quad (11)$$

$$\delta N_{se2} = a_1{}^2\delta T_2 + a_2{}^2\delta N_1 + a_3{}^2\delta T_e + a_4{}^2\delta\Sigma, \quad (11')$$

where $a_1{}^1 = \partial N_{se}/\partial T_2$, $a_2{}^1 = \partial N_{se}/\partial N_1$, $a_3{}^1 = \partial N_{se}/\partial T_e$, $a_4{}^1 = \partial N_{se}/\partial\Sigma$, $a_1{}^2 = \partial N_{se2}/\partial T_2$, $a_2{}^2 = \partial N_{se2}/\partial N_1$, $a_3{}^2 = \partial N_{se2}/\partial T_e$, and $a_4{}^2 = \partial N_{se2}/\partial\Sigma$. $a_1{}^1$, $a_2{}^1$, $a_3{}^1$, and $a_4{}^1$ are evaluated at N_{se1}, $a_1{}^2$, $a_2{}^2$, $a_3{}^2$, and $a_4{}^2$ are evaluated at N_{se2}, and the rms error $\delta\Sigma$ is expressed as

$$\delta\Sigma = \left[\frac{\left(\frac{\delta\Delta}{\delta\Delta_0}\right)^2 + \left(\frac{\delta\psi}{\delta\psi_0}\right)^2 + \left(\frac{\delta\phi_0}{\delta\phi_{00}}\right)^2 + \left(\frac{\delta N_s}{\delta N_{s0}}\right)^2 + \left(\frac{\delta K_s}{\delta K_{s0}}\right)^2 + \left(\frac{\delta N_0}{\delta N_{00}}\right)^2}{6}\right]^{1/2},$$

where $\delta\Delta_0$, $\delta\psi_0$, $\delta\phi_{00}$, δN_{s0}, δK_{s0}, and δN_{00} are 1°/24, 1°/12, 0.02°, 0.008, 0.008, and 0.0003, respectively, as given in Table 1. Substituting the expressions given by Eqs. (11) and (11′) into Eq. (10), we obtain the total error, δK_1:

$$\delta K_1 = \gamma(b_1{}^1 - b_1{}^2)\delta T_2 + \gamma(b_2{}^1 - b_2{}^2)\delta N_1 + \gamma(b_3{}^1 - b_3{}^2)\delta T_e + \gamma(b_4{}^1 - b_4{}^2)\delta\Sigma, \quad (12)$$

where $b_i{}^1 = a_i{}^1/(N_{se1} - N_1)$ and $b_i{}^2 = a_i{}^2/(N_{se2} - N_1)$ for $i = 1, 2, 3, 4$. In Eq. (12) the parameters γ, $b_1{}^1$, $b_1{}^2$, $\ldots$, $b_4{}^1$, and $b_4{}^2$ can be numerically computed and used to estimate the error δK_1 if there are deviations occurring in T_2, N_1, T_e, and Σ. Table 2 lists a set of $b_1{}^1$, $b_1{}^2$, $b_2{}^1$, $b_2{}^2$, $\ldots$, $b_4{}^1$, and $b_4{}^2$ values that are evaluated for T_1 in the thickness range 1000–3000 Å, assuming that $\hat{N}_1 = 3.80 - i0.05$, $N_2 = 1.46$, and $T_2 = 200$ Å. From Table 2 it is found that $b_1{}^1$, $b_2{}^1$, $b_3{}^1$, and $b_4{}^1$ are nearly equal to $b_1{}^2$, $b_2{}^2$, $b_3{}^2$, and $b_4{}^2$, respectively. In other words, $b_1{}^1 - b_1{}^2$, $b_2{}^1 - b_2{}^2$, $b_3{}^1 - b_3{}^2$, and $b_4{}^1 - b_4{}^2$ are very small. This indicates that the error for K_1 is reduced.

By using Eq. (12) the percentage errors, δK_1 (%), caused by each parameter can be computed in terms of T_2, the thickness of the sandwiched SiO_2 layer, and the results are shown in Fig. 6(a). In this computation, two $N_{se}(\max)$'s and two

Table 2. Error Sensitivity Parameters Used to Compute the Error dK_1 for $\hat{N}_1 = 3.80 - i0.05$, $N_2 = 1.46$, $T_2 = 200$ Å, and T_1 between 1000 and 3000 Å

b_1^1	b_1^2	b_2^1	b_2^2	b_3^1	b_3^2	b_4^1	b_4^2
5.554×10^{-3}	5.509×10^{-3}	1.682	1.553	-4.188×10^{-4}	-4.591×10^{-4}	1.574×10^{-2}	1.473×10^{-2}

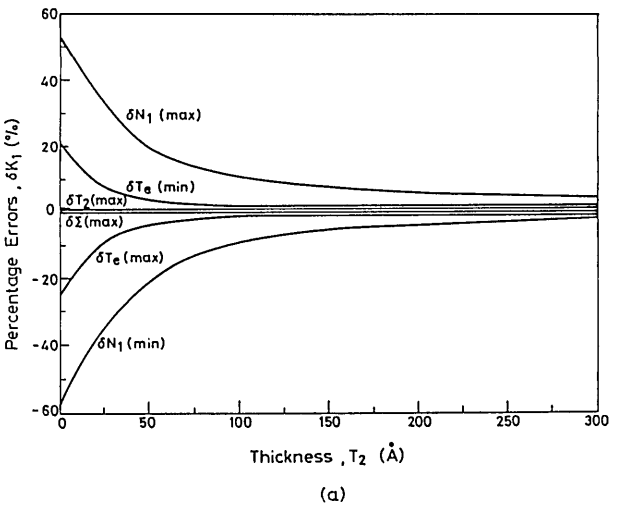

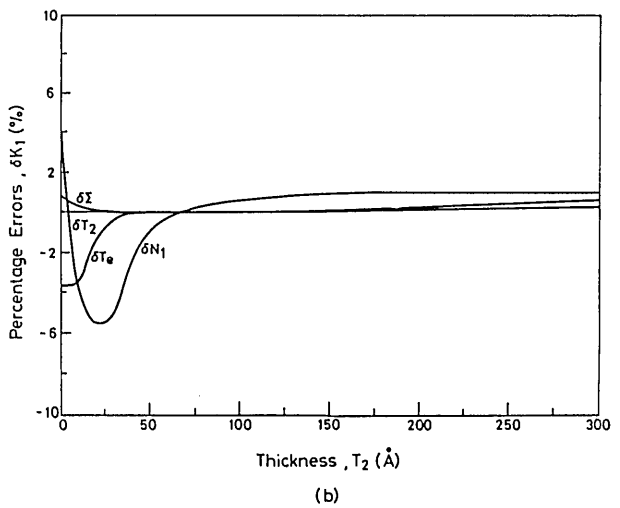

Fig. 6. (a) Plots of the percentage errors in K_1 derived with the proposed method in terms of the thickness, T_2, that are due to various small deviations of $\delta\Sigma$, δN_1, δT_2, and δT_e. δN_1(max), δT_2(max), $\delta\Sigma$(max), and δT_e(max) are determined from the maximum points, and δN_1(min) and δT_e(min) are determined from the minimum points, in the $N_{se} - T$ plot. For the computation, $N_1 = 3.80 - i0.05$, $N_2 = 1.46 - i0.00$, and T_1 is between 1000 and 3000 Å. (b) Same as (a), but here the average values of the curves of (a) are taken.

N_{se}(min)'s are used to compute K_1. The N_{se}(max) and N_{se}(min) are chosen in the thickness range 1000–3000 Å. From Fig. 6(a) it is seen that the error δK_1 is a function of the thickness T_2. As T_2 increases above 150 Å, all curves approach the zero-error axis. Among all the parameters, N_1 is the most significant parameter and suffers the largest error. The errors computed through N_{se}(max) and N_{se}(min) are symmetric with respect to the zero-error axis. Hence, if the K_1 value is obtained by averaging the value computed by using N_{se}(max) and the value computed by using N_{se}(min), the errors can be averaged out. The errors after this averaging procedure is used are shown in Fig. 6(b). They are small and generally can be neglected. Compare Fig. 6(b) with Fig. 3; it is shown that the error in determining K_1 is much reduced when this method is used.

Analysis of Errors in the Determination of N_1

From Eq. (7′) the errors δN_1 can be expressed, if the $\delta(\Delta N)$ term is neglected, as

$$\delta N_1 = \frac{\delta N_{se}(\max) + \delta N_{se}(\min)}{2}. \tag{13}$$

Also, δN_{se}(max) and δN_{se}(min) can be expressed in terms of the deviations of each parameter as

$$\delta N_{se}(\max) = c_1\delta T_2 + c_2\delta K_1 + c_3\delta T_e + c_4\delta\Sigma, \tag{14}$$

$$\delta N_{se}(\min) = c_1'\delta T_2 + c_2'\delta K_1 + c_3'\delta T_3 + c_4'\delta\Sigma, \tag{14'}$$

where $c_1 = \partial N_{se}/\partial T_2$, $c_2 = \partial N_{se}/\partial K_1$, $c_3 = \partial N_{se}/\partial T_e$, $c_4 = \partial N_{se}/\partial\Sigma$, $c_1' = \partial N_{se}'/\partial T_2$, $c_2' = \partial N_{se}'/\partial K_1$, $c_3' = \partial N_{se}'/\partial T_e$, and $c_4' = \partial N_{se}'/\partial\Sigma$. c_1, c_2, c_3, and c_4 are evaluated at N_{se}(max), and c_1', c_2', c_3', and c_4' are evaluated at N_{se}(min). Substituting Eqs. (14) and (14′) into Eq. (13) gives δN_1 as

$$\delta N_1 = \left(\frac{c_1 + c_1'}{2}\right)\delta T_2 + \left(\frac{c_2 + c_2'}{2}\right)\delta K_1 + \left(\frac{c_3 + c_3'}{2}\right)\delta T_e + \left(\frac{c_4 + c_4'}{2}\right)\delta\Sigma. \tag{15}$$

Similarly, δN_1 can be evaluated by computing $c_1, c_1', \ldots, c_4$, and c_4'. A set of $c_1, c_1', \ldots, c_4$, and c_4' is computed and listed in Table 3, where $c_1, c_1', \ldots, c_4$ and c_4' are evaluated for T_1 in the thickness range 1000–3000 Å by assuming that $\hat{N}_1 = 3.80 - i0.05$, $N_2 = 1.46$, and $T_2 = 200$ Å. From this table it can be seen that $(c_1 + c_1')$, $(c_2 + c_2')$, $(c_3 + c_3')$, and $(c_4 + c_4')$ may be small since c_1, c_2', and c_4 are positive but c_1', c_2, and c_4' are negative and both c_3 and c_3' are small. Hence the errors are

Table 3. Error Sensitivity Parameters Used to Compute the Error dN_1 for $\hat{N}_1 = 3.80 - i0.05$, $N_2 = 1.46$, $T_2 = 200$ Å, and T_1 between 1000 and 3000 Å

c_1	c_1'	c_2	c_2'	c_3	c_3'	c_4	c_4'
6.401×10^{-3}	-4.191×10^{-3}	−6.952	5.232	-4.646×10^{-4}	-4.785×10^{-4}	6.501×10^{-3}	-1.874×10^{-3}

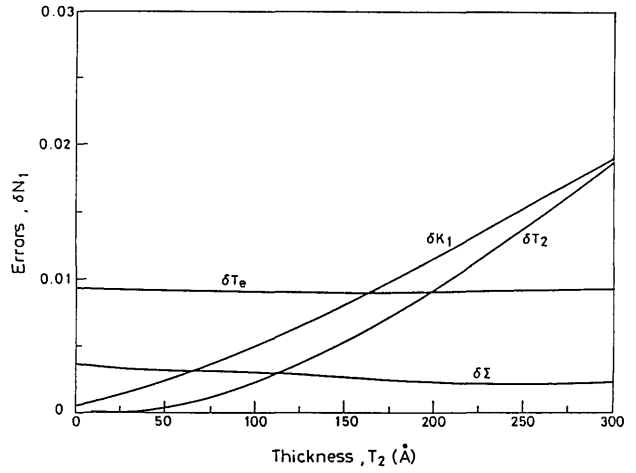

Fig. 7. Plots of the errors in N_1 derived with the proposed method in terms of the thickness, T_2, that are due to various small deviations of $\delta\Sigma$, δK_1, δT_2, and δT_e. For the computation, $\hat{N}_1 = 3.80 - i0.05$, $N_2 = 1.46 - i0.00$, and T_1 is between 1000 and 3000 Å.

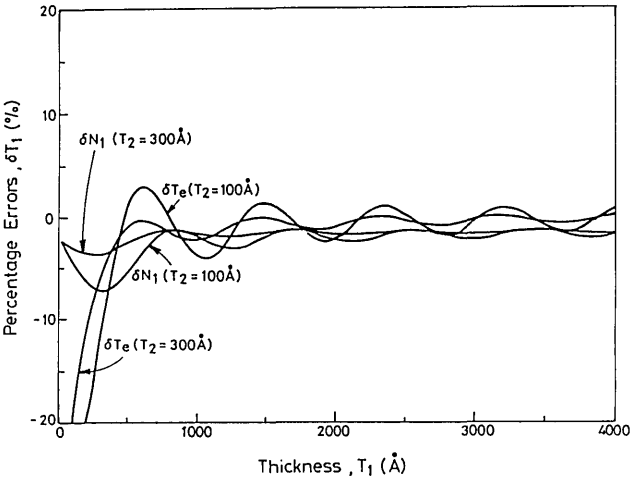

Fig. 8. Plots of percentage errors in the thickness, T_1, due to various small deviations of δN_1 and δT_e for $\hat{N}_1 = 3.80 - i0.05$ and for $T_2 = 100$ Å and $T_2 = 300$ Å, respectively.

reduced. By using Eq. (15), the errors δN_1 caused by each parameter are also computed for $\hat{N}_1 = 3.80 - i0.05$ in terms of T_2, and the results are shown in Fig. 7. It is seen that δN_1 increases with T_2. However, for T_2 less than 300 Å, δN_1 is less than 0.02, which is acceptable. Comparing Fig. 7 with Fig. 2 shows that the error in determining N_1 by using this method is much reduced.

Analysis of Errors in the Determination of T_1

According to Eqs. (1) and (2), if N_1 and K_1 have been determined, the thickness, T_1, can be computed. It is interesting to know the error introduced in computing T_1. In this section the errors in determining T_1 are also analyzed.

In Fig. 8 the percentage errors δT_1 caused by δT_e and δN_1 for $T_2 = 100$ Å and $T = 300$ Å, respectively, are plotted versus T_1 for $N_1 = 3.80 - i0.05$. The errors caused by all other parameters such as Δ, ψ, ϕ_0, N_s, and K_s are small and thus are not plotted in the figure. It can be seen that the errors are generally less than 5% for a poly-Si thickness larger than 500 Å. When $T_2 = 100$ Å and $T = 300$ Å are compared, the errors for the 300-Å case are smaller than those for the 100-Å case. Hence, if the oxide sandwiched between the silicon substrate and the poly-Si layer is chosen to be 300 Å (or larger), the errors in determining N_1, K_1, and T_1 are generally negligible.

EXPERIMENTAL RESULTS

The proposed method has been applied to measure the refractive index of poly-Si films. The experimental details are described in this section, and the measured refractive index is related to the processing conditions for poly-Si films.

Experimental Details

In order to obtain many data on various thicknesses of measured films in order to derive the $N_{se} - T_1$ plot, samples with a beveled surface were used. The samples were prepared by first thermally growing a layer of oxide of 300–500-Å thickness of on a 3–5-Ω/cm, ⟨100⟩ silicon wafer. A poly-Si film whose refractive index was to be measured was then deposited upon the wafer by chemical-vapor deposition. The deposited poly-Si film was then put into a plasma etcher, and a specially made movable shutter was inserted into the etcher to etch the surface of the poly-Si film into a beveled surface. The light beam of the ellipsometer (Rudolph AutoEL-III) was scanned across the beveled surface. The (Δ, ψ) data corresponding to different thicknesses were then obtained. The $N_{se} - T_1$ diagrams were computed by using Eqs. (3) and (4).

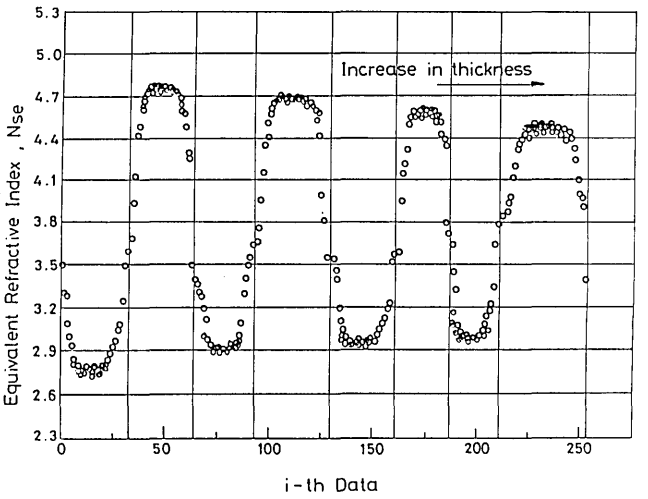

Fig. 9. Plot of N_{se} as a function of the sequence of measurement data for the experimental wafer with a beveled surface on the poly-Si film.

Table 4. Set of Measured N_{se}(max) and N_{se}(min) Values Used to Compute N_1 and K_1

N_{se}(max)	N_{se}(min)	Results
4.771	2.801	$N_1 = 3.708$
4.674	2.919	$K_1 = 0.049$
4.598	2.970	
4.492	2.995	

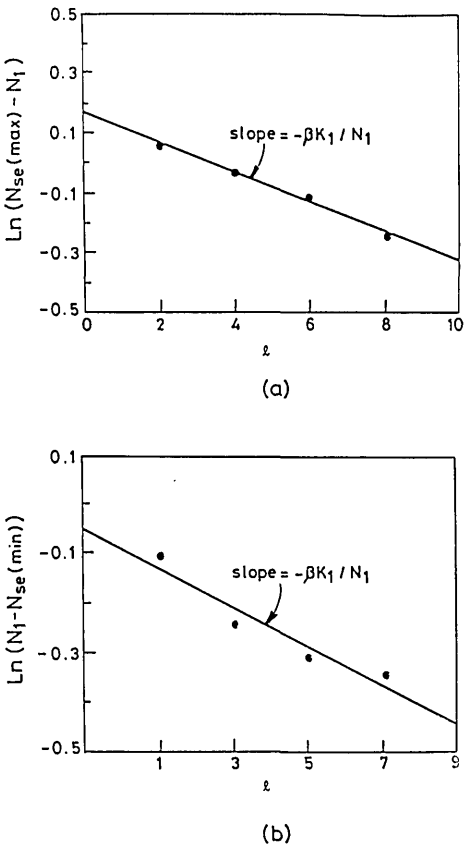

Fig. 10. Least-squares fittings for plots of (a) $\ln[N_{se}(\max) - N_1]$ versus l and (b) $\ln[N_1 - N_{se}(\min)]$ versus l, from the computed N_{se} values in Fig. 9. l is the number of the maximum point or the minimum point. The slopes in the fitted curves give the $-\beta K_1/N_1$ value.

Measured Refractive Index ($N_1 - iK_1$) of Polycrystalline-Silicon Films

Figure 9 is an example of the $N_{se} - T_1$ plot computed from the data obtained experimentally for a poly-Si film deposited upon a 207-Å SiO_2 film. In this figure N_{se} is plotted in terms of the sequence of data instead of the thickness T_1. It is because only $N_{se}(\max)$ and $N_{se}(\min)$ are needed for computing N_1 and K_1 and the film thicknesses do not need to be computed. For this measurement, the thickness range of the beveled surface of the poly-Si film was 1500–6000 Å. There are four $N_{se}(\max)$'s and four $N_{se}(\min)$'s in the figure, and their values are listed in Table 4. The $N_{se}(\max)$ and $N_{se}(\min)$ values decrease in amplitude with the film thickness. N_1 and K_1 were obtained by using the following numerical iteration procedure: A K_1 value was estimated to fit the experimental curve of Fig. 9 to obtain an N_1 value. The N_1 value obtained was then used to plot the $\ln[N_{se}(\max) - N_1]$- and $\ln[N_1 - N_{se}(\min)]$-versus-l plots (Fig. 10) to derive a new value for K_1. This new K_1 value was compared with the previously estimated K_1 value. If these two K_1 values differed significantly, the K_1 value derived later was used to fit the curve of Fig. 9 again. A new N_1 value was obtained. This new N_1 value was used to derive K_1 again. This process was repeated four times, and the newly derived K_1 value differed from the previous K_1 value within 0.0001. The final N_1 and K_1 values were taken as the true values. The N_1 and K_1 values obtained were 3.708 and 0.049, respectively. Figure 10 shows the final $\ln[N_{se}(\max) - N_1]$- and $\ln[N_1 - N_{se}(\min)]$-versus-l plots for this iteration process.

It is assumed that the N_1 and K_1 values of the poly-Si film are highly sensitive to the process by which the poly-Si film is prepared. N_1 and K_1 of the poly-Si films that have been subjected to different processing conditions have been measured, and the results are described below.

Figures 11(a) and 11(b) show the measured N_1 and K_1, respectively, for poly-Si films deposited at different deposition temperatures. The figures show that the higher deposition temperature produces poly-Si films with lower N_1's and K_1's. The measured value of N_1 for films deposited at the low temperature is closer to that of single-crystal silicon. However, the value of K_1 for the higher deposition temperature is closer to that of single-crystal silicon.

The effects of annealing on N_1 and K_1 of the poly-Si film have also been studied. The measured values of N_1 and K_1 in terms of the annealing time are shown in Figs. 12(a) and 12(b), respectively, where A, B, and C represent samples whose deposition temperatures were 570, 610, and 650°C, respectively. In this experiment annealing was performed at 1000°C in a nitrogen ambient. In general, for samples prepared at deposition temperatures of 610 and 650°C, the changes in N_1 and K_1 are insignificant with respect to the annealing time. For the 570°C samples, N_1 and K_1 drop with the annealing time. In particular, the K_1 value changes significantly and becomes saturated to the value of single-

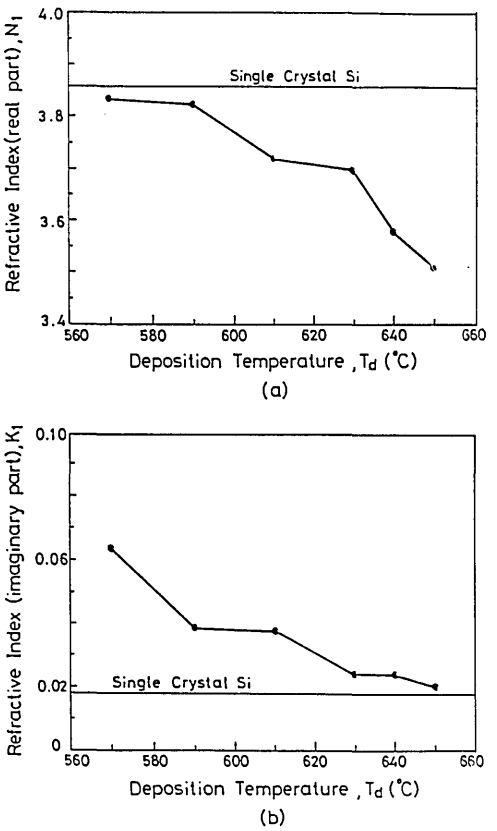

Fig. 11. (a) Real part of the refractive index, N_1, as a function of the deposition temperature, T_d, for experimental as-grown poly-Si films. (b) The imaginary part of the refractive index, K_1.

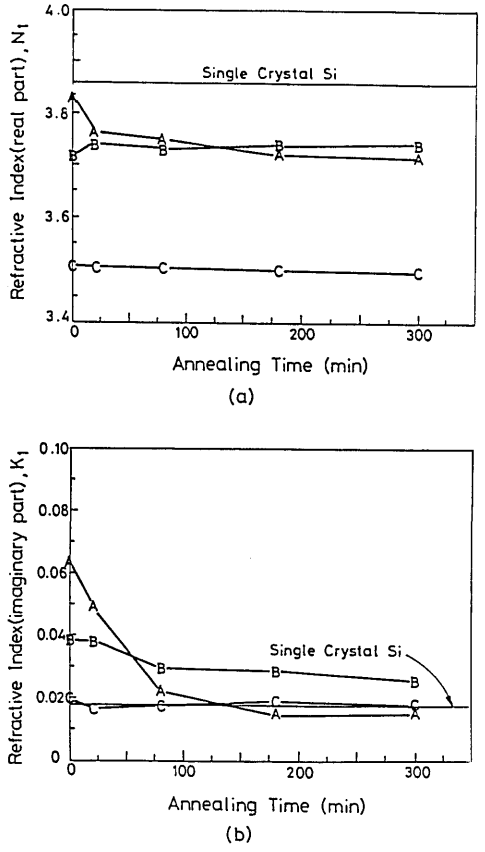

Fig. 12. (a) Real part of the refractive index, N_1, as a function of the annealing time for experimental as-grown poly-Si films. (b) The imaginary part of the refractive index, K_1.

crystal silicon. From these two figures it appears that the annealing process does not affect the refractive indices of poly-Si films deposited at a temperature higher than 610°C.

CONCLUSIONS

The above analyses have shown that the conventional ellipsometry method used to measure the complex refractive index $N_1 - iK_1$ of poly-Si films is highly sensitive to small deviations in ellipsometric parameters; thus large errors could occur during measurement and computation. Furthermore, as the thickness of the measured film is close to the half-period of the ellipsometric cycle, the errors will become too large to make the measurement meaningful. A new scheme, which is to compute the $N_{se} - T_1$ plot based on the zero-layer model, has been proposed to reduce the error sensitivities over the most sensitive parameters of T_2, N_1, and T_e during computation of K_1, and over the most sensitive parameters of T_2, K_1, and T_e during computation of N_1. In this method, N_1 is computed by averaging the neighboring N_{se}(max) and N_{se}(min) values in the $N_{se} - T_1$ plot. K_1 is determined through $\ln[N_{se}(\max) - N_1]$- and $\ln[N_1 - N_{se}(\min)]$-versus-l plots. Error analyses have shown that the error in this method can be reduced by at least an order of magnitude.

As N_1 and K_1 are substituted in computations of the thickness T_1, the errors can be reduced to minimum if a SiO_2 layer with a thickness larger than 300 Å is sandwiched between the substrate and the layer of the film whose thickness is to be computed.

This method has been applied to measure the refractive index of low-pressure chemical-vapor-deposition poly-Si films. It was found that, for the poly-Si films prepared at the higher deposition temperature, N_1 and K_1 of the deposited films are lower in value. For films deposited at temperatures higher than 570°C, the annealing process (1000°C in a nitrogen ambient) does not affect their refractive indices.

For this paper all the computations were done for $N_1 = 3.80 - i0.05$ in a thickness range of 0–4000 Å. However, this method can be applied to any materials with any other refractive indices and thicknesses.

APPENDIX A: DERIVATION OF N_{se}(max) AND N_{se}(min)

The ellipsometric relationship between the measurable parameters, Δ and ψ, and the sample parameters can be expressed as[12]

$$\tan \psi e^{i\Delta} = \frac{r_p}{r_s}, \tag{A1}$$

where r_p and r_s are the complex reflection coefficients for light parallel and perpendicular, respectively, to the incident plane. For the zero-layer model of Fig. 4(b), $T_1 = 0$, and Eq. (A1) becomes

$$\tan \psi e^{i\Delta} = \frac{r_{2p}''}{r_{2s}''}, \tag{A2}$$

where

$$r_{2p}'' = \frac{(N_{se} - iK_{se})^2 \cos(\phi_0) - [(N_{se} - iK_{se})^2 - \sin^2(\phi_0)]^{1/2}}{(N_{se} - iK_{se})^2 \cos(\phi_0) + [(N_{se} - iK_{se})^2 - \sin^2(\phi_0)]^{1/2}} \tag{A2'}$$

and

$$r_{2s}'' = \frac{\cos(\phi_0) - [(N_{se} - iK_{se})^2 - \sin^2(\phi_0)]^{1/2}}{\cos(\phi_0) + [(N_{se} - iK_{se})^2 - \sin^2(\phi_0)]^{1/2}}. \tag{A2''}$$

In the single-layer model, the ratio of the reflection coefficients, r_p/r_s, can be expressed in terms of sample parameters as[12]

$$\frac{r_p}{r_s} = \frac{[r_{1p} + r_{2p} \exp(-i2\delta_1)][1 + r_{1s} r_{2s} \exp(-i2\delta_1)]}{[1 + r_{1p} r_{2p} \exp(-i2\delta_1)][r_{1s} + r_{2s} \exp(-i2\delta_1)]}, \tag{A3}$$

where r_{1p} (r_{1s}) and r_{2p} (r_{2s}) are the reflection coefficients between the ambient medium and the surface layer (the surface layer and the substrate) for light parallel (perpendicular) to the incident plane. The complex phase shift is defined by

$$\delta_1 = (2\pi/\lambda)\hat{N}_1 T_1 \cos(\phi_1), \tag{A4}$$

where $\phi_1 = \sin^{-1}[N_0 \sin(\phi_0)/N_1]$. If the expression for r_p/r_s given by Eq. (A3) is substituted into Eq. (A1) and the $\tan \psi e^{i\Delta}$ obtained is substituted into Eq. (A2), the following equation is obtained:

$$\frac{r_{2p}''}{r_{2s}''} = \frac{[r_{1p} + r_{2p}\exp(-i2\delta_1)][1 + r_{1s}r_{2s}\exp(-i2\delta_1)]}{[1 + r_{1p}r_{2p}\exp(-i2\delta_1)][r_{1s} + r_{2s}\exp(-i2\delta_1)]}. \quad \text{(A5)}$$

Equation (A5) is the basic formula used to derive the $N_{se} - T_1$ plot. If the refractive index of the surface layer is close to that of the substrate, the equation can be simplified, and the maximum or minimum N_{se} of the $N_{se} - T_1$ plot can be derived as follows:

According to Eqs. (A2′) and (A2″), if $|N_{se} - iK_{se}| \gg \sin(\phi_0)$, and $|N_{se} - iK_{se}| \gg \cos(\phi_0)$, the following approximations are obtained:

$$r_{2p}'' \cong \frac{N_{se}\cos(\phi_0) - 1 - iK_{se}\cos(\phi_0)}{N_{se}\cos(\phi_0) + 1 - iK_{se}\cos(\phi_0)}, \quad \text{(A6)}$$

$$r_{2s}'' \cong -1, \quad \text{(A7)}$$

and

$$\frac{r_{2p}''}{r_{2s}''} \cong \frac{-N_{se}\cos(\phi_0) + 1 + iK_{se}\cos(\phi_0)}{N_{se}\cos(\phi_0) + 1 - iK_{se}\cos(\phi_0)}. \quad \text{(A8)}$$

Substituting approximation (A8) into Eq. (A5), we have

$$\frac{-N_{se}\cos(\phi_0) + 1 + iK_{se}\cos(\phi_0)}{N_{se}\cos(\phi_0) + 1 - iK_{se}\cos(\phi_0)} = \frac{[r_{1p} + r_{2p}\exp(-i2\delta_1)][1 + r_{1s}r_{2s}\exp(-i2\delta_1)]}{[1 + r_{1p}r_{2p}\exp(-i2\delta_1)][r_{1s} + r_{2s}\exp(-i2\delta_1)]}. \quad \text{(A9)}$$

In Eq. (A4), if $|N_1 - iK_1| \gg \sin(\phi_0)$, δ_1 is reduced to

$$\delta_1 \cong \pi\frac{T_1}{p}(1 - iw), \quad \text{(A10)}$$

where

$$p = \frac{\lambda}{2}\frac{1}{[N_1^2 - \sin^2(\phi_0)]^{1/2}}, \qquad w = \frac{N_1K_1}{[N_1^2 - \sin^2(\phi_0)]}.$$

Substituting the expression for δ_1 in approximation (A10) into Eq. (A9), we obtain

$$\frac{-N_{se}\cos(\phi_0) + 1 + iK_{se}\cos(\phi_0)}{N_{se}\cos(\phi_0) + 1 - iK_{se}\cos(\phi_0)} = \frac{r_{1p} + \alpha_1\exp(-i2\pi T_1/p)\exp(-2\pi T_1w/p)}{r_{1s} + \alpha_2\exp(-i2\pi T_1/p)\exp(-2\pi T_1w/p)}, \quad \text{(A11)}$$

where $\alpha_1 = r_{1p}r_{1s}r_{2s} + r_{2p}$ and $\alpha_2 = r_{1s}r_{1p}r_{2p} + r_{2s}$. Differentiating Eq. (A11), we obtain the following approximation:

$$-i2\pi\exp(-2\pi T_1w/p) \times \frac{[\cos(2\pi T_1/p) - i\sin(2\pi T_1/p)](\alpha_1r_{1s} - \alpha_2r_{1p})}{p[r_{1s} + \alpha_2\exp(-i2\pi T_1/p)\exp(-2\pi T_1\delta/p)]^2}\,dT_1 = \frac{-2\cos(\phi_0)dN_{se} + i2\cos(\phi_0)dK_{se}}{[1 + N_{se}\cos(\phi_0) - iK_{se}\cos(\phi_0)]^2}. \quad \text{(A12)}$$

Taking the real part on both sides of Eq. (A12), and letting $dN_{se}/dT_1 = 0$, which is the condition for the local maximum or the local minimum in the $N_{se} - T_1$ plot, we obtain approximately

$$\pi\exp(-2\pi T_1w/p)\sin\left(\frac{2\pi T_1}{p}\right)\frac{(\alpha_1r_{1s} - \alpha_2r_{1p})}{pr_{1s}^2\cos(\phi_0)} \times [1 + N_{se}\cos(\phi_0)]^2 = 0. \quad \text{(A13)}$$

Since $\alpha_1r_{1s} - \alpha_2r_{1p} \neq 0$, this leads to $\sin(2\pi T_1/p) = 0$. That is,

$$2\pi T_1/p = m\pi \quad \text{or} \quad T_1 = m\frac{p}{2}, \qquad m = 0, 1, 2, 3, \ldots. \quad \text{(A14)}$$

Substituting $T_1 = mp/2$ into approximation (A7) and assuming that $w \cong K_1/N_1$, we obtain the approximate expression

$$\frac{r_{1p} + \alpha_1\exp(-im\pi)\exp(-m\pi K_1/N_1)}{r_{1s} + \alpha_2\exp(-im\pi)\exp(-m\pi K_1/N_1)} = \frac{-N_{se}\cos(\phi_0) + 1 + iK_{se}\cos(\phi_0)}{N_{se}\cos(\phi_0) + 1 - iK_{se}\cos(\phi_0)}. \quad \text{(A15)}$$

If m is even [i.e., $m = 2l$ for $l = 0, 1, 2, \ldots$, which is the condition for N_{se} to be the local maximum in the $N_{se} - T_1$ plot], Eq. (A15) becomes

$$\frac{r_{1p} + \alpha_1\exp(-2l\pi K_1/N_1)}{r_{1s} + \alpha_2\exp(-2l\pi K_1/N_1)} = \frac{-N_{se}\cos(\phi_0) + 1 + iK_{se}\cos(\phi_0)}{N_{se}\cos(\phi_0) + 1 - iK_{se}\cos(\phi_0)}. \quad \text{(A16)}$$

Using the identity $(A - B)/(A + B) = (C - D)/(C + D)$ if $A/B = C/D$, we simplify Eq. (A16) to

$$\frac{(r_{1p} - r_{1s}) + (\alpha_1 - \alpha_2)\exp(-2l\pi K_1/N_1)}{r_{1p} + r_{1s}) + (\alpha_1 + \alpha_2)\exp(-2l\pi K_1/N_1)} = \frac{-2N_{se}\cos(\phi_0) + i2K_{se}\cos(\phi_0)}{2}. \quad \text{(A17)}$$

Because $\phi_1 \cong \phi_2$ if $N_1 \cong N_2$ in the single-layer model, the following approximate relationships are valid:

$$r_{1p} = \frac{N_1\cos(\phi_0) - N_0\cos(\phi_1)}{N_1\cos(\phi_0) + N_0\cos(\phi_1)}, \qquad r_{1s} = -1,$$

$$r_{2p} = \frac{N_2 - N_1}{2N_1}, \qquad r_{2s} = \frac{N_1 - N_2}{2N_1},$$

$$\alpha_1 = r_{1p}r_{1s}r_{2s} + r_{2p} = r_{2p}(r_{1p} + 1), \qquad \alpha_2 = r_{1s}r_{1p}r_{2p} + r_{2s}$$
$$= -r_{2p}(r_{1p} + 1), \qquad \alpha_1 + \alpha_2 = 0, \qquad \alpha_1 - \alpha_2$$
$$= 2r_{2p}(r_{1p} + 1), \qquad \cos(\phi_1) = \cos(\phi_2) = 1.$$

Substituting the above relationships into Eq. (A17), neglecting the K_{se} term, and assuming that $N_0 = 1$, we obtain

$$-N_1\cos(\phi_0)\left[1 + \frac{N_2 - N_1}{N_1}\exp(-2l\pi K_1/N_1)\right] = -N_{se}\cos(\phi_0) \qquad \text{for } l = 0, 1, 2, \ldots \quad \text{(A18)}$$

or

$$N_{se} = N_1 + (N_2 - N_1)\exp(-2l\pi K_1/N_1) \qquad \text{for } l = 0, 1, 2, \ldots, \quad \text{(A18′)}$$

which can be written as

$$N_{se}(\max) = N_1 + (N_s - N_1)\exp[-2(m-1)\pi K_1/N_1] \quad \text{for } m = 1, 2, 3, \ldots, \quad \text{(A19)}$$

where N_s is the refractive index (real part) of the substrate. Similarly, the local minimum N_{se} can also be derived:

$$N_{se}(\min) = N_1 - (N_s - N_1)\exp[-(2m-1)\pi K_1/N_1] \quad \text{for } m = 1, 2, 3, \ldots. \quad \text{(A19}')$$

REFERENCES

1. M. Hirose, M. Taniguchi, and Y. Osaka, "Electronic properties of chemically deposited polycrystalline silicon," J. Appl. Phys. **50**, 377–382 (1979).
2. G. Harbeke, L. Krausbauer, E. F. Steingmeier, and A. E. Widmer, "LPCVD polycrystalline silicon: growth and physical properties of *in-situ* phosphorus doped and undoped films," RCA Rev. **44**, 287–293 (1983).
3. M. T. Duffy, J. T. McGinn, J. M. Shaw, R. T. Smith, and R. A. Soltis, "LPCVD polycrystalline silicon: growth and physical properties of diffusion-doped, ion-implanted, and undoped films," RCA Rev. **44**, 313–325 (1983).
4. G. Harbeke, L. Krausbauer, E. F. Steigmeier, and A. E. Widmer, "Growth and physical properties of LPCVD polycrystalline silicon films," J. Electrochem. Soc. **131**, 675–682 (1984).
5. R. M. A. Azzam and N. M. Bashara, *Ellipsometry and Polarized Light* (North-Holland, Amsterdam, 1977).
6. R. F. Spanier, "Double film thickness measurements in the semiconductor industry," in *Integrated Circuit Metrology I*, D. Nyyssonen, ed., Proc. Soc. Photo-Opt. Instrum. Eng. **342**, 109–120 (1982).
7. C. J. Dell'Oca, "Nondestructive thickness determination of polycrystalline silicon deposited on oxidized silicon," J. Electrochem. Soc. **119**, 108–111 (1972).
8. J. H. Ho, C. L. Lee, C. W. Jen, and T. F. Lei, "Ellipsometry measurement on SiO_2 films for thickness under 200 Å," Solid State Electron. **30**, 973–981 (1987).
9. J. H. Ho, C. L. Lee, and T. F. Lei, "Error reduction in the ellipsometric measurement on thin transparent film," Solid State Electron. **31**, 1321–1326 (1988).
10. D. A. Holmes and D. L. Feucht, "Theory of an ellipsometric technique for investigating weakly absorbing substrates," J. Opt. Soc. Am. **57**, 755–757 (1967).
11. E. A. Irene and D. W. Dong, "Ellipsometry measurements of polycrystalline silicon films," J. Electrochem. Soc. **129**, 1347–1353 (1982).
12. S. So Samuel, "Ellipsometric analysis for an absorbing surface film on an absorbing substrate with or without an intermediate surface layer," Surf. Sci. **56**, 97–108 (1976).